



# Energy management of the energy storage-based micro-grid-connected system: an SOGSNN strategy

Kallol Roy<sup>1</sup> · Kamal Krishna Mandal<sup>2</sup> · Atis Chandra Mandal<sup>3</sup>

Published online: 9 October 2019  
© Springer-Verlag GmbH Germany, part of Springer Nature 2019

## Abstract

In this paper, a novel hybrid algorithm is implemented for the system modelling and the optimal management of the micro-grid (MG)-connected systems with low cost. The increasing number of renewable energy sources and distributed generators requires new strategies for their operations in order to maintain the energy balance between the renewable sources and MG. Therefore, an efficient hybrid technique is proposed in the paper. The main objective of the process was the optimum operation of micro-sources for decreasing the electricity production cost by hourly day-ahead and real-time scheduling. The proposed hybrid technique is to manage the power flows between the energy sources and the grid. To achieve this point, demand response and minimum cost of energy are determined. The proposed hybrid technique is the combined performance of both the gravitational search algorithm (GSA)-based artificial neural network (ANN) and squirrel search algorithm (SSA), and it is named as SOGSNN. This technique is involved with the mathematical optimization problems that necessitate more than one fitness function to be optimized simultaneously. By using the inputs of MG-like wind turbine, photovoltaic array, fuel cell, micro-turbine, diesel generator and battery storage with corresponding cost functions, the GSA-based ANN learning phase is employed to predict the load demand. SSA clarifies the squirrel in optimizing the configuration of MG based on the load demand. The proposed hybrid technique is implemented in MATLAB/Simulink working platform and compared with other solution techniques like ANFASO method. The comparison result reveals that the superiority of the proposed technique confirms its ability to solve the problem.

**Keywords** Battery · Cost function · DG · FC · Load demand · MG · MT · PV · SOGSNN · WT

## 1 Introduction

Electric power distribution systems are considered as the promising concepts for the next generation (Kaundinya et al. 2009). Constantly delivering power and extending nature of demand is the difficult and challenging task for the developed and developing countries. Usage of power, exhaustible nature of petroleum derivatives and the

increasing state of environment have made interest in renewable energy sources (RESs) (Dali et al. 2010; Ahmed et al. 2008). The RESs like solar and wind energy are non-depletable and non-polluting, are littler in estimate, and can be installed nearer to load centres and attainable (Deshmukh and Deshmukh 2008). The growth of wind and photovoltaic (PV) power generation systems has exceeded the most optimistic estimation. For consumers, a multi-source hybrid alternative energy system is higher than a single resource based on the higher reliability and power quality in multi-source hybrid alternative energy system (Dursun and Kilic 2012; Hajizadeh and Golkar 2007). The integrated approach makes a hybrid system more appropriate for isolated communities, for example remote islands (Bajpai and Dash 2012; Palizban et al. 2014). In the upcoming generation, the distribution network will need smart grid ideas (Figueiredo and Martins 2010). Flexible micro-grids (MGs) are able to work in all the ecological conditions. For both grid-connected and

---

Communicated by V. Loia.

✉ Kallol Roy  
kallolroy0181@gmail.com

<sup>1</sup> University Institute of Technology, Burdwan University, Bardhaman, West Bengal, India

<sup>2</sup> Power Engineering Department, Jadavpur University, Kolkata, West Bengal, India

<sup>3</sup> Physics Department, Burdwan University, Bardhaman, West Bengal, India

stand-alone applications, controllers are more suitable for being developed and implemented in inverters (Gu et al. 2014).

Both grid-associated and stand-alone applications are being created and executed in inverters which could support the hybrid system operation. Different control techniques guarantee MG systems operation which also explores the topologies of high-end converter and inverter. The conventional droop-based, centralized and master-slave controllers are utilized for the demand of high-bandwidth communication system (Vasquez et al. 2010; Prakash and Sinha 2014, Pavan Kumar and Ravikumar 2016; Roy et al. 2016). Execution of weak transient, when load dynamic is included, results in stability lack and black-start ability lack which are the drawbacks in the controllers (Elsied et al. 2016). Different strategies are executed to overcome the previously mentioned challenges. The methods are fuzzy-logic-based controller (Thao and Uchida 2016), hierarchical control scheme (Najafzadeh and Heydari 2012), sliding mode control and neuro-fuzzy control (Golsorkhi and Lu 2015; Moradi et al. 2017). The previously mentioned systems do not totally bring about less steady-state tracking error and better robustness. Furthermore, when large-signal disturbances happen, these procedures are not worth for constraining the current, i.e. starting condition of motor or fault occurs in SC that may trip out unit of DER or harm the components (Prakash and Sinha 2014). The proposed strategy is obviously portrayed in detail. The rest of this article is listed as follows: the recent research work and the background of the research work are discussed in Sect. 2. The proposed technique is carefully clarified in Sect. 3. The proposed technique's achievement results and the related discussions are given in Sect. 4, and the paper is concluded in Sect. 5.

## 2 Recent research works: a brief review

Different research works have already existed in the literature which depended on the unit commitment with a renewable system utilizing different methods and different viewpoints. A portion of the works is reviewed here.

A hybrid methodology for the cost of production minimization, renewable energy resources' better use and programming ideal operation of electrical systems has been executed by Roy et al. (2018). Here, BFOA (bacterial foraging optimization algorithm) and ANN (artificial neural network) techniques were employed in their research methodology. Moradi et al. (2018) have represented a stand-alone micro-grid with optimal energy scheduling under uncertainties of the system. So as to get energy resource use efficiently, a battery storage system was presented for the management of energy. In the plan of online

management of power flow, a design and experimental validation of system energy management were contributed by Luna et al. (2018). In micro-grid, MOPSO methods for the management of energy and optimal energy resources' distribution have been displayed by Aghajani and Ghadimi (2018). To demonstrate the exhibited strategy adequacy, the strategy was contrasted by the NSGA-II system.

Sharma et al. (2018) have set up a 2-m point estimate method (PEM) which is connected to model the load demand uncertainties, prices in the market and RES available power in MG to limit the MG's aggregate operation cost in the presence of BES by considering MG uncertainties. To limit the MG operation cost, SIMBO-Q (swine influenza model-based optimization with quarantine) and WOA (whale optimization algorithm) have been connected. Indragandhi et al. (2018) have considered solving the problems such as the price of the system and QoS (quality of service) with the hybrid micro-grid configuration. These primarily focused on the management of power flow in AC/DC micro-grid, and its optimization has been examined using a multi-objective particle swarm optimization (MOPSO) algorithm. Goroochi Sardou et al. (2018) have illuminated a robust model of particle swarm optimization (PSO), and PDIP (primal-dual interior point) method was introduced for optimal management of micro-grid energy flow considering PV inverters with VAR compensation mode. To respond to various necessities, a hybrid energy storage system (HESS) containing both high-energy and power density storage battery bank and ultra-capacitor unit was established by Aktas et al. (2018). For a hybrid energy storage system (HESS) supplied from 3-phase 4-wire grid-connected photovoltaic (PV) power system, a new smart energy management algorithm (SEMA) was presented by Aktas et al. (2019). In an AC micro-grid, a new convex model predictive control strategy for dynamic optimal power flow between battery energy storage systems distributed was elucidated by Thomas Morstyn et al. (2018). Comprehensive control and power management system (CAPMS) for PV-battery-based hybrid micro-grids with both AC and DC buses, for both grid-connected and islanded modes, was introduced by Yi et al. (2018).

### 2.1 Background of the research work

The recent research work shows that the management of distributed energy with micro-grid is one of the multi-objective problems in energy management. Because perfect economic model of energy source of micro-grid units is needed to describe the operating cost taking into report the output power generated, the constraints of the multi-objective optimization problem are transformed into an easier sub-problem that can be solved and used as the basis of an

iterative process. From the previous works, it has been found that the optimum dispatch strategy is affected by various parameters, such as fuel cost, fuel conversion efficiency of the generator, operation and maintenance (O&M) costs, renewable penetration, and battery and generator capacity. Moreover, various techniques are used for energy management strategies, such as bacterial foraging optimization algorithm (BFOA), artificial neural network (ANN), whale optimization algorithm (WOA), swine influenza model-based optimization with quarantine (SIMBO-Q) and so on. Utilizing BFOA gives better outcomes; however, it easily suffers from the partial optimism and it cannot work out the scattering problems. ANN can model difficult functions and can be imposed on any application. But it exhibits some limitations like large complexity of structure. The neural network needs the training to operate. Then again, WOA has easier implementation and has a tendency to produce solutions near the best individual value for every objective. But the limitation in WOA is that each solution is evaluated only with respect to one objective. To track the power demand, a renewable energy system control strategies are mainly designed optimally to use energy sources. To overcome these challenges, an incorporated MG system is required for a promising arrangement. In the literature, not many strategies-based works are displayed to deal with this issue; these disadvantages and issues have motivated to do this research work. The proposed method with MG architecture is illustrated in the accompanying segment 3.

### 3 Architecture of MG-connected system with the proposed controller

The proposed controller is actualized to the MG-connected system architecture which is delineated in Fig. 1. The MG-connected system contains a collection of radial feeders; the feeders are associated with the sensitive and non-sensitive loads and PCC (point of common coupling), i.e. single connection point, power and voltage (P&V) controller.

The feeders additionally have micro-sources, for example, wind turbine (WT), photovoltaic (PV), diesel generator (DG), fuel cell (FC) and micro-turbine (MT) (Roy and Mandal 2014). Moreover, the micro-sources in the feeder, for example, DG, MT and FC, need fuel for generating the power. Other than the WT and PV, there is no need for any other fuels; the power generation process is carried out from nature, because these sources are renewable energy sources. Static switch is utilized to island the feeder from the utility if any event occurs. Whenever unexpected contingences occur, the breaker is utilized to

avoid the system reparation. With the utilization of MGs and the battery storage, the entire structure is used to solve the power demand issue. To limit the depth of discharging, the battery requires a charge controller. It additionally limits the charging current supply to the battery and prevents the battery from overcharging. The power generated from all the MGs is utilized to serve the load as well as to charge the battery. With the use of the WT and PV, the required load demand is mostly utilized due to the free generation cost. Whenever it does not fulfil the condition, the DG, FC and MT are utilized for solving the problem. Figure 1 demonstrates that the power generated from all the micro-sources can be directed to serve the load and to charge the battery (Mohamed and Koivo 2007). The general form of these relationships is expressed below:

$$p_i = p_{i,\text{load}} + p_{i,\text{battery}}, \quad \forall i = 1, 2, \dots, N, \quad (1)$$

where  $p_i$  represents the output power from generator unit  $i$ ,  $p_{i,\text{load}}$  represents the power from generator unit  $i$  to serve the load,  $p_{i,\text{battery}}$  represents the power from generator unit  $i$  to charge the battery, and  $N$  is the number of generators.

#### 3.1 Multi-objective function of the proposed methodology

The selected configuration of the MG should fulfil the load demand with a minimum fuel cost, operation and maintenance cost. So the DG, FC and MT fuel cost functions are considered as the multi-objective function. The multi-objective function is determined as (2):

$$F_{\text{obj}} = \min_{i=1}^4 \{F_i(c)\}, \quad (2)$$

where  $F_{\text{obj}}$  is the multi-objective function to minimize the fuel cost, operation and maintenance cost of the MG-connected system and  $F_i(c)$  represents the total fuel cost of MG models:

$$F_1(c) = \sum_{i=1}^N a_i + b_i P_{\text{DG},i} + c_i P_{\text{DG},i}^2, \quad (3)$$

where  $F_1(c)$  is the fuel cost of DG,  $a_i$ ,  $b_i$  and  $c_i$  are the fuel coefficients with  $i = 1, 2, \dots, n$ ,  $N$  is the number of generators, and  $P_{\text{DG},i}$  is the output power of the generator.

$$F_2(c) = c_{\text{NG}} \sum_{\text{FC}} \frac{P_{\text{FC}}}{\eta_{\text{FC}}}, \quad (4)$$

where  $F_2(c)$  is the fuel cost of FC,  $P_{\text{FC}}$  is the output power of the FC,  $\eta_{\text{FC}}$  is the efficiency of the FC, and  $c_{\text{NG}}$  is the natural gas price of the FC. The efficiency of the FC is  $\eta_{\text{FC}} = 0.47$ .

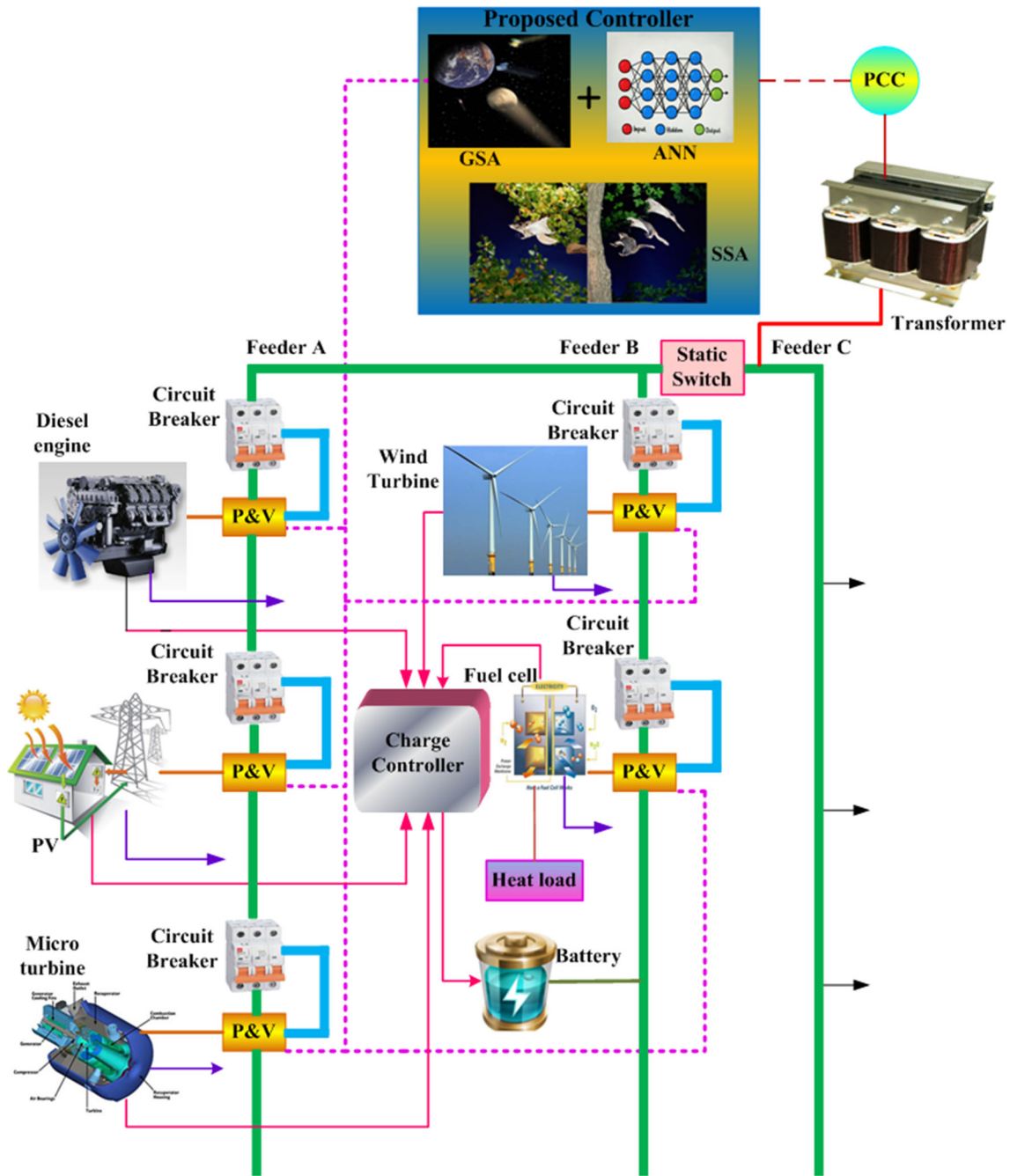


Fig. 1 Architecture of MG-connected systems with the proposed controller

$$F_3(c) = \sum_{MT} \frac{f_{NG} P_{MT}}{\eta_{MT}}, \tag{5}$$

where  $F_3(c)$  is the fuel cost of MT,  $P_{MT}$  is the output power of the MT,  $\eta_{MT}$  is the efficiency of the MT, and  $f_{NG}$  is the natural gas price of the MT. The efficiency of the MT is  $\eta_{MT} = 0.47$ .

$$F_4(c) = \sum_{i=1}^N (c_i f_i + om_i) + \sum_{i=1}^N \sum_{j=1}^M \alpha_j (ef_{ij} P_j), \tag{6}$$

where  $c_i$  represents the fuel cost of the generating unit in Rs/L for the diesel and Rs/kWh for the natural gas,  $f_i$  indicates the fuel consumption rate of a generating unit,  $om_i$  represents the operation and maintenance cost of a generating unit,  $\alpha_j$  is the externality cost of emission type  $j$ ,  $N$  is the number of generating units,  $M$  represents the number of generating units, and  $ef_{ij}$  is the emission factor of the generating unit.

### 3.2 Load demand prediction using gravitational search algorithm (GSA)-based artificial neural network (ANN) technique

The first stage of the proposed hybrid technique is depicted in this section. The hybrid technique is the joined execution of both GSA and ANN techniques. The proposed hybrid technique is utilized here to meet the renewable available energy power and to keep up the grid power demand from the grid operator. ANN is a universal method to portray the processes in a logical form. The motivation beyond the algorithm is the elementary components called “neurons”. With the corresponding input time intervals, here we are training the ANN using the target power demand. GSA is utilized for ANN learning phase (Muralitharan et al. 2018). Gravitational search algorithm is a recently and a meta-heuristic optimization algorithm created by Rashedi et al. (2009). This algorithm, which is motivated by the Newton’s famous law of gravity and the law of motion, has a great potential to be a breakthrough optimization method. By the gravity force, all these objects are attracted each other and towards the objects with the heavier masses; this force causes a global movement of all objects. To predict the load demand, the GSA-based ANN learning phase is employed here. And furthermore it compares the local best and global best solution. The ANN network model is made out of input layer, hidden layer and output layer. Each layer is provided with a feedforward connection. The network is trained with the historical data set which is the previous year demand data set. The demand variation for every hour is represented as input data set which trains the network of ANN. Subsequently, it generates the optimal demand output, according to the load; the demand for each hour is varied. The GSA is adopted for training the neural network which is given as below.

#### 3.2.1 Steps of GSA

GSA, as a meta-heuristic algorithm, is generated by the concepts of gravity. Here, the random generation of positions of agents is initialized within the given search interval. To solve the issue, GSA is utilized. The best found solution is adjusted by the local search process, i.e. pattern search. The GSA operators are implied, and agents move in the search space at the start of each iteration. For some iteration, this serial combination is repeated.

##### Step 1: Initialization

In this step, initialize the population array of particles with input as time interval and the output as the power demand.

##### Step 2: Random Generation

After the initialization process, randomly generate the initialized input parameters of the system.

$$\text{random}^i = \begin{bmatrix} p_d^{11} & p_d^{12} & \dots & p_d^{1n} \\ p_d^{21} & p_d^{22} & \dots & p_d^{2n} \\ \vdots & \vdots & \vdots & \vdots \\ p_d^{m1} & p_d^{m2} & \dots & p_d^{mn} \end{bmatrix}. \tag{7}$$

Here,  $p_d$  represents the power demand.

##### Step 3: Fitness

In order to predict the optimal load demand, the fitness functions for all agents are done. The fitness is computed and described as follows:

$$\text{Error}, e = \frac{1}{2} \sum (t_D - d_D), \tag{8}$$

where  $d_D$  is the desired output demand and  $t_D$  is the target output demand.

##### Step 4: Gravitational Constant Computation

Using the  $t$  iteration by ensuing Eq. (11), the gravitational constant  $g(t)$  is computed.

$$g(t) = g_0 \exp\left[-\alpha \frac{t}{I}\right], \tag{9}$$

where  $g_0$  represents the gravitational constant chosen randomly,  $\alpha$  is the constant,  $t$  is the current era, and  $I$  indicates the total iteration number.

##### Step 5: Inertial Mass Updation

The inertial mass and the gravitational constant are updated by subsequent iteration, and it is derived as follows:

$$Mg_j(t) = \frac{\text{Fit}_j(t) - W(t)}{B(t) - W(t)}. \tag{10}$$

The following equation shows the mass of the  $j$ th agent:

$$mg_j(t) = \frac{mg_j(t)}{\sum_{i=1}^n mg_j(t)}. \tag{11}$$

##### Step 6: Total Mass Calculation

The evaluation of the total force acting on the  $j$ th agent at iteration  $t$  is given as follows:

$$F_j^d(t) = \sum_{i \in kB, i \neq j} \text{rand}_i F_{ji}^d(t), \tag{12}$$

where  $\text{rand}_i$  represents the random number between interval  $[0, 1]$  and the set of first  $K$  agents is  $kB$  with the best fitness value and biggest mass.  $F_{ji}^d(t)$  is the force acting on the  $j$ th mass from the  $i$ th mass.

##### Step 7: Acceleration and Velocity

Through the law of gravity and law of motion, the acceleration  $A_j^d(t)$  at iteration  $t$  and the velocity  $V_j^d(t+1)$  of the  $j$ th agent at next iteration  $t+1$  in  $d$ th dimension are updated.



$$A_j^d(t) = \frac{F_j^d(t)}{\text{mg}_j^d(t)} \quad (13)$$

$$V_j^d(t+1) = \text{rand}_j \times V_j^d(t) + A_j^d(t). \quad (14)$$

### Step 8: Agent's Position Update

Then, the next positions of  $j$ th agents in  $d$ th dimension of the agents are updated using the accompanying equation:

$$X_j^d(t+1) = X_j^d(t) + V_j^d(t+1). \quad (15)$$

### Step 9: Termination

Until the iteration achieves their maximum limit, the steps from 3 to 9 are repeated. At the final iteration, the best solutions of algorithm are computed as a global fitness function of the problem and at specified dimensions the position of the corresponding agent as the global solution of that problem. The best solution is selected in the termination stage based on the fitness function. The best value of the optimization process is represented as  $e^{\text{best}}$  and  $p_d^{\text{best}}$ . The best data set of the optimization parameters is defined as follows:

$$\begin{bmatrix} e^{11} & e^{12} & \dots & e^{1n} \\ e^{21} & e^{22} & \dots & e^{2n} \\ \vdots & \vdots & \vdots & \vdots \\ e^{m1} & e^{m2} & \dots & e^{mn} \end{bmatrix} = \begin{bmatrix} p_d^{11} & p_d^{12} & \dots & p_d^{1n} \\ p_d^{21} & p_d^{22} & \dots & p_d^{2n} \\ \vdots & \vdots & \vdots & \vdots \\ p_d^{m1} & p_d^{m2} & \dots & p_d^{mn} \end{bmatrix} \quad (16)$$

Therefore, the best combination of error signals and the power demand can be demonstrated.

## 3.2.2 Steps of ANN

**Step 1:** The input vector  $b$  is applied in the network input layer. Then, the equation for the input vector  $b$  can be expressed as:

$$b = \{b_1, b_2, b_3, \dots, b_n\}^t. \quad (17)$$

The net input for the  $j$ th hidden unit is given by

$$N_j^h = \sum_{i=1}^n w_{ji} b_i + \beta_j^h, \quad (18)$$

where  $w_{ji}$  is the weight on the connection from the  $i$ th input unit and  $\beta_j^h$  is the bias for neuron's hidden layer for  $j = 1, 2, \dots, h$ .

**Step 2:** The output of the neurons in the hidden layer is written as follows:

$$H_j^h = f \left( \sum_{i=1}^n w_{ji} b_i + \beta_j^h \right). \quad (19)$$

The net input to the neurons in the output layer becomes

$$O_k^o = \sum_{j=1}^{m_h} w_{jk} b_j + \beta_k^o. \quad (20)$$

**Step 3:** Finally, the output neurons, i.e. actual output of the feedforward loop  $\chi_a$  in the output layer, are equated as follows:

$$H_k^o = f \left( \sum_{j=1}^{n_h} w_{jk} b_j + \beta_k^o \right). \quad (21)$$

**Step 4:** The ANN learning stage is performed by updating the weights and biases using back-propagation algorithm in order to minimize a mean-squared-error (MSE) performance index which is given as

$$e = \min \left\{ \frac{1}{2} (\chi_o - \chi_t)^2 \right\}, \quad (22)$$

where  $\chi_t$  is the target output value and  $\chi_a$  is the actual output value of ANN.

**Step 5:** Expressions of updating for the synaptic weights are given as follows:

$$w_{ji}(n+1) = w_{ji}(n) - \varsigma \left( \frac{\partial e}{\partial w_{ji}(n)} \right) + \xi \Delta w_{ji}(n) \quad (23)$$

$$\Delta w_{ji}(n) = w_{ji}(n) - w_{ji}(n-1) \quad (24)$$

where  $\varsigma$  is the learning factor and momentum factor is  $\xi$ . The controller can be utilized to determine the optimum configuration of the MG combinations based on the load demand once the above-mentioned process is completed. The GSA-based ANN technique is used to predict the load demand in the MG-connected systems; it can be briefly described in Sect. 3.3.

## 3.3 Optimal configuration of MG-connected system using squirrel search algorithm (SSA)

This section clarifies the squirrel in optimizing the configuration of micro-grid in the light of load demand. For optimizing the configuration of MG-connected system with minimum of fuel cost, i.e. MT, FC and DG fuel cost functions, the multi-objective function is required. In SSA, load demand is taken as the input and the output is the combination of MG-connected systems. SSA is a new simple and powerful nature-inspired searching algorithm for unconstrained numerical optimization problems created by Jain et al. (2018). The dynamic foraging behaviour of southern flying squirrels is simulated using this algorithm. The efficient way of locomotion of this algorithm is known as gliding. This algorithm totally clarifies each and every feature of its food search. The algorithm steps to optimize the configuration of the MG-connected systems are quickly clarified as follows.

### 3.3.1 Layers of SSA algorithm

#### Layer 1: Initialization

Initialize the load demand as the input and MG-connected systems such as WT, PV, DG, FC, MT, cost functions and corresponding generation limits as output.

#### Layer 2: Random Generation

In this layer, randomly generate the  $n$  number of flying squirrels in a forest and location of  $i$ th flying squirrel can be indicated by a vector. The location of all flying squirrels can be represented as follows:

$$fs = \begin{bmatrix} fs_{1,1} & fs_{1,1} & \cdots & \cdots & fs_{1,1} \\ fs_{1,1} & fs_{1,1} & \cdots & \cdots & fs_{1,1} \\ \vdots & \vdots & \vdots & \vdots & \vdots \\ \vdots & \vdots & \vdots & \vdots & \vdots \\ fs_{1,1} & fs_{1,1} & \cdots & \cdots & fs_{1,1} \end{bmatrix}, \tag{25}$$

where  $fs_{i,j}$  indicates the  $j$ th dimension of  $i$ th flying squirrel. To allocate the initial location of each flying squirrel in the forest, a uniform distribution is utilized.

$$fs_i = fs_l + U(0, 1) \times (fs_u - fs_l), \tag{26}$$

where  $fs_l$  and  $fs_u$  are lower and upper bounds, respectively, of  $i$ th flying squirrel in  $j$ th dimension and  $U(0, 1)$  is a uniformly distributed random number in the range of  $[0, 1]$ .

#### Layer 3: Fitness Function

Location of each flying squirrel is figured and estimated through the fitness function. The multi-objective function is inferred as follows:

$$\text{Fitness Function} = \text{Min}\{cf_1, cf_2, cf_3, cf_4\} \tag{27}$$

where  $cf_1$  is the cost function of DG,  $cf_2$  is the fuel cell cost function,  $cf_3$  is the MT cost function, and  $cf_4$  represents the operation and maintenance cost.

#### Layer 4: Sorting Declaration and Random selection

The array is sorted in ascending order after storing the fitness values of each flying squirrel's location. The flying squirrel with minimum fitness value is declared on the hickory nut tree. Then, the next best flying squirrels are contemplated to be on the acorn nut trees and are supposed to move towards hickory nut tree. The remaining flying squirrels are expected to be on normal tree. Some squirrels are examined to move towards hickory nut tree, expecting that they have fulfilled their daily food requirements. The remaining squirrels will proceed to acorn nut trees to meet their daily energy need. By the presence of predators, the foraging behaviour of flying squirrels is always affected. By employing the location updating mechanism with

predator presence probability ( $P_{DP}$ ), the natural behaviour is modelled.

#### Layer 5: New Location Generation

Three situations may occur during the dynamic foraging of flying squirrels as discussed previously. In each situation, it is assumed that in the absence of predator, flying squirrels glide and search efficiently throughout the forest for their favourite food. Otherwise, if the predator is present, flying squirrels use small random walk to search a nearby hiding location. The mathematical model for the dynamic foraging behaviour is calculated as follows: it consists of three cases:

**Case 1:** Flying squirrels on acorn nut trees ( $fs_{at}$ ) may move towards hickory nut tree. In this case, new locations of squirrels can be given as follows:

$$fs_{at}^{t+1} = \begin{cases} fs_{at}^t + d_G \times g_c \times (fs_{ht}^t - fs_{at}^t) & r_1 \geq P_{DP} \\ \text{Random Location} & \text{Otherwise} \end{cases}, \tag{28}$$

where  $d_G$  represents the random gliding distance. With the help of gliding constant  $g_c$  in the mathematical model, the balance between exploration and exploitation is achieved,  $fs_{ht}^t$  represents the location of flying squirrel that reached hickory nut tree,  $t$  denotes the current iteration, and  $r_1$  is the random number in the range of  $[0, 1]$ .

**Case 2:** Flying squirrels on acorn nut trees ( $fs_{nt}$ ) may move towards acorn nut trees to fulfil their daily energy needs. In this case, new locations of squirrels can be calculated as follows:

$$fs_{nt}^{t+1} = \begin{cases} fs_{nt}^t + d_G \times g_c \times (fs_{nt}^t - fs_{nt}^t) & r_2 \geq P_{DP} \\ \text{Random Location} & \text{Otherwise} \end{cases}, \tag{29}$$

where  $r_2$  is the random number in the range of  $[0, 1]$ .

**Case 3:** Some squirrels on normal trees and already utilized acorn nuts may move to hickory nut tree in order to store hickory nuts at the time of scarcity. In this case, new locations of squirrels can be determined as follows:

$$fs_{nt}^{t+1} = \begin{cases} fs_{nt}^t + d_G \times g_c \times (fs_{ht}^t - fs_{nt}^t) & r_3 \geq P_{DP} \\ \text{Random Location} & \text{Otherwise} \end{cases}, \tag{30}$$

where  $r_3$  is the random number in the range of  $[0, 1]$ .  $P_{DP}$  is the predator presence probability, and the value of  $P_{DP}$  in all cases is 0.01.

#### Layer 6: Aerodynamics of Gliding

By equilibrium gliding in which the sum of lift ( $L$ ) and drag ( $D$ ) force produces a resultant force ( $R$ ) whose magnitude is equal and opposite to the direction of flying

squirrel's weight, gliding mechanism of flying squirrels is explained. The approximated gliding distance  $d_G$  is derived as follows:

$$d_G = \left( \frac{h_G}{\tan \phi} \right), \quad (31)$$

where  $h_G = 8$  m which is the loss in height occurred after gliding.

#### Layer 7: Seasonal Monitoring Condition

In SSA, seasonal monitoring condition prevents it from being in local optimal solutions. The following equation shows the seasonal monitoring condition, i.e.  $s_c < s_{\min}$ .

$$s_{\min} = \frac{10E^{-6}}{(365)^{m/2.5}}, \quad (32)$$

where  $s_c$  is the seasonal constant,  $s_{\min}$  represents the minimum value of seasonal constant, and  $t$  and  $t_m$  are the current and maximum iteration values, respectively. The value  $s_{\min}$  affects the exploration and exploitation capabilities. The larger value of  $s_{\min}$  promotes exploration, and the lower value of  $s_{\min}$  enhances the exploitation capability. Due to these actions, the gliding constant is utilized. If seasonal monitoring condition is found true, relocation of flying squirrels can be updated.

#### Layer 8: Random Relocation

The relocation of such flying squirrels is modelled through the following equation:

$$f_{s_{nt}}^{\text{new}} = f_{s_L} + \text{Le} \cdot \text{vy}(n) \times (f_{s_u} - f_{s_l}) \quad (33)$$

where Levy distribution encourages better and efficient search space exploration.

#### Layer 9: Stopping Criterion

Check the stopping criterion is satisfied. If it is not satisfied go to step 5, else terminate the search.

Therefore, the system is able to provide the optimal MG configuration with minimum fuel cost, operation and maintenance cost once the above process is completed. The proposed hybrid technique structure is depicted in Fig. 2. Section 4 explains that the proposed method is implemented in MATLAB/Simulink platform, and the obtained results are compared with the existing techniques.

## 4 Results and discussion

In this paper, a hybrid technique is presented for minimizing the total generation cost and maximizing the power. To meet the system load demand, PV, WT and battery sources have been utilized. From the proposed technique, the increased demand has been met using the optimal

configuration of MG sources. The GSA-based ANN technique is utilized to predict the load demand in the MG-connected systems. SSA illuminates the squirrel in optimizing the configuration of micro-grid based on the load demand. This technique is actualized in MATLAB/Simulink, and their performance level is tested with other solution techniques. The parameters of energy resources are given in Table 1.

### 4.1 Analysis of power generation

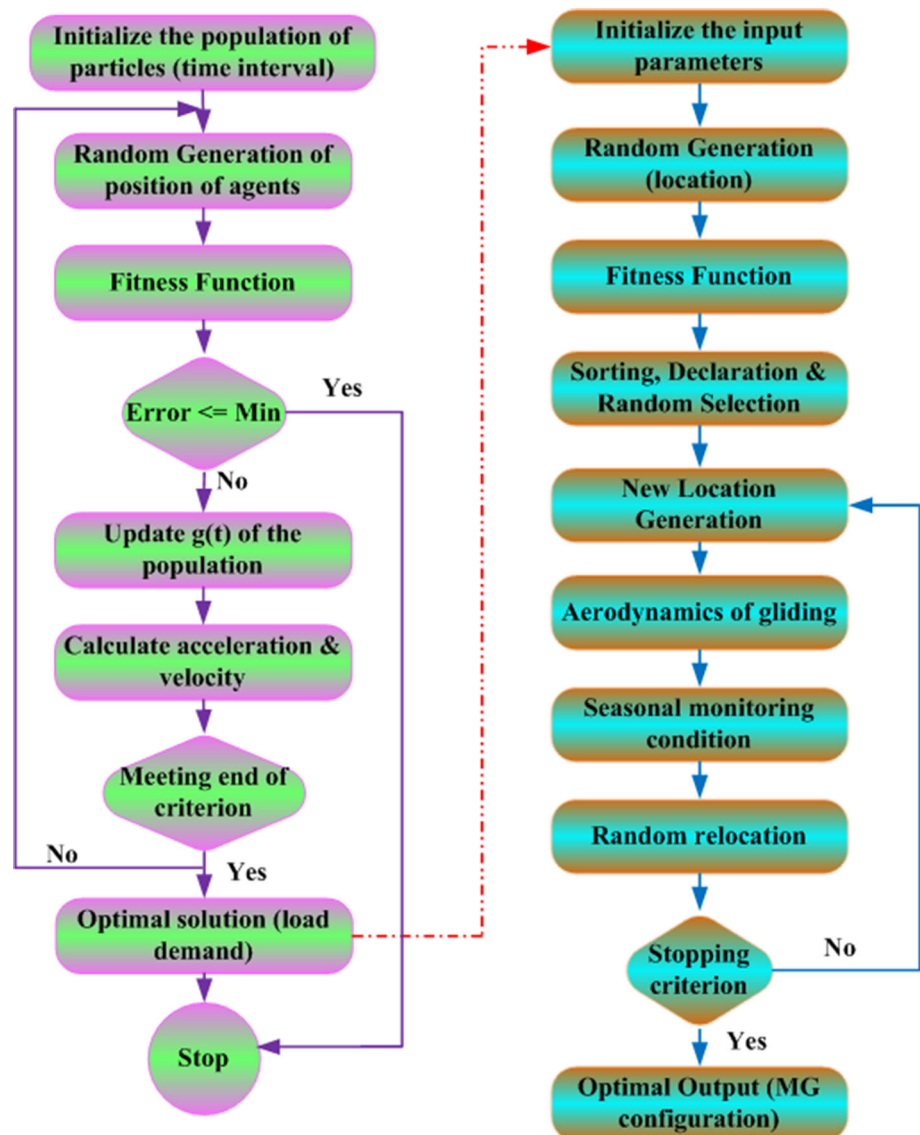
The MG's combination of optimal configuration and the corresponding total cost using existing techniques is shown in Table 2. Figure 3 shows the analysis of generated power by battery, MT, PV and WT.

As it is observed from Fig. 3a during the initial period, in the time period 1–12 h, the battery is charged. In the discharge mode of battery, at the time moment 12–16 h, the battery power is utilized. In any case, MT is utilized for the power needed for charging the battery. Figure 3b demonstrates that the generated power of MT is analysed in 24 h. It reaches the maximum power of 12 kW in the specific time moment of  $t = 8$ –17 h. Figure 3c demonstrates that the generated power of PV is executed in 24 h. The PV has achieved the maximum power of 2.5 kW in the time moment of  $t = 1$ –7 h. In the peak hours at the time moment  $t = 8$ –17 h, it is raised up to 5.8 kW. After the moment of time,  $t = 18$ –24 h, the power produced by PV decreased up to 0.65 kW. Figure 3d shows that the penetrated power of WT is examined in 24 h. In the time moment  $t = 1$ –7 h while analysing the wind power, the generated power is decreased from 3.5 to 2.5 kW. At the time moment  $t = 8$ –17 h, the power is increased to 7.6 kW. Again, the power decreased in the time moment of  $t = 18$ –24 h; the power value varies from 5.2 to 1.8 kW.

Figure 4 clearly shows the analysis of power generation for various sources. Figure 4a illustrates that during the initial period, in the time period 1–12 h, the battery is charged. In the discharge mode of battery, at the moment of time 12–16 h, the battery power is utilized. However, MT is utilized for the power required for charging the battery. Figure 4b demonstrates that the generated power of MT is analysed in 24 h. It reaches the maximum power of 12 kW in the particular time moment of  $t = 8$ –17 h. Figure 4c shows that the generated power of PV is executed in 24 h. The PV has attained the maximum power of 2.5 kW in the time moment of  $t = 1$ –7 h. In the peak hours at the time moment  $t = 8$ –17 h, it is raised up to 5.8 kW. After the moment of time,  $t = 18$ –24 h, the power generated by PV decreased up to 0.65 kW. Figure 4d displays that the penetrated power of WT is analysed in 24 h. In the time moment  $t = 1$ –7 h while analysing the wind power, the generated power is decreased from 3.5 to 2.5 kW. At the



**Fig. 2** Flow chart of GSA-ANN and SSA



time moment  $t = 8\text{--}17$  h, the power is increased to 7.6 kW. Again, the power reduced in the time moment of  $t = 18\text{--}24$  h; the power value varies from 5.2 to 1.8 kW. The overall analysis of power generated from the sources utilizing the proposed technique is more proficient than that the utilizing the ANFASO method.

## 4.2 Analysis of SOC

In Fig. 5, the analysis of state of charge (SOC) using the proposed and ANFASO methods is discussed. During the normal operation, the system can meet all the power demands by the load the proposed algorithm MT is assisted. If the MG is not able to completely supply the load demand, battery is fully discharged. During the time instant 18–24 h, battery is operated in discharging mode reaching SOC. At the specific time intervals, the battery operates in

the charging mode. By proper selection of MT, battery is operated in the charging mode with the proposed algorithm and the SOC is reached about 85%.

## 4.3 Analysis of cost

The cost of operation is identified with the renewable energy sources, and the battery under charging and discharging mode is watched for 24 h keeping in mind the end goal to deal with the MG-connected system. Figure 6 shows the comparison analysis of the cost of the proposed technique with existing techniques. It clearly elucidates that the proposed method gives low cost when compared with existing techniques. In all the current methods, the aggregate cost of the MG-connected system is high which is seen from the figure. In charging mode, the BS is worked in more often than not and in the time scope of 1 to 12 h it

**Table 1** Parameters of energy resources

Resources	Description	Ranges
WT	Wind speed	5.7
	Cut-in speed	3.5
	Cut-out speed	18
	Rated speed	17.5
PV	Irradiance	1000
	Temperature	25
	Cell temperature	55
Battery	System voltage	200
	Capacity	6.5
	SOC max	100
DG	Di	0.4333
	Ei	0.2333
	Fi	0.0074
FC	Cost	0.00175

**Table 2** Optimal MG combination selection using different techniques

Load demand (KW)	3.5	5.5	8.3	10.8	13.5
FC (KW)	0.00	1.50	4.00	4.00	4.00
MT (KW)	3.50	4.00	4.00	4.00	4.00
WT (KW)	0.00	0.00	0.30	2.80	5.50
Total cost (\$/h)					
ABC	0.72	1.21	2.49	3.25	4.16
BFO	0.63	1.12	2.39	3.04	3.95
ANFASO	0.55	1.10	1.91	2.50	3.70
Proposed	0.31	1.01	1.86	2.12	3.49

is primarily focused. BS is generally discharging, amid whatever is left of the period. On comparing with ABC, BFA and ANFASO strategy, the aggregate cost is abundantly lessened on using the proposed approach.

In order to evaluate the effectiveness of the proposed method, the elapsed time is evaluated and compared with ANFASO which is displayed in Table 3. It is seen from the table that the proposed techniques achieve less computation time when compared with ANFASO. In order to show the capability of the proposed approach, the MCP of the proposed technique is analysed with ANFASO technique. The mean, median and standard deviation of the proposed technique are 1.991, 1.998 and 0.735, respectively, which are lower than those of the ANFASO technique displayed in Table 4. Figure 6 shows the comparison analysis of the cost of the proposed technique with existing techniques. It clearly elucidates that the proposed method gives low cost when compared with existing techniques. The proposed method adequacy can be computed in the light of the estimation of cost accuracy percentage (ECAP), and the condition is detailed as takes after (27):

$$ECAP = \frac{\text{best-worst}}{\text{best}} \times 100 \quad (27)$$

In the light of the condition (27), the percentage accuracy of the proposed and various techniques is resolved. Table 5 demonstrates the execution comparison of the proposed technique with various techniques.

From Table 5, we have observed that the percentage accuracy of the different techniques has low ECAP. Be that as it may, the proposed technique is high and more optimal than the different techniques. The ECAP estimation of the proposed technique is 10.25%. A different existing technique, for example, ABC, BFO, ANFASO and the comparable load demand, is connected, and the total cost is resolved. The proposed method's viability has been demonstrated in the comparative results. Comparison analysis of SoC using various methods is shown in Table 6. The percentage of SoC of the proposed technique is higher than that of the existing techniques. The SoC of the proposed technique is 82%, ABC is 78%, BFO is 70% and ANFASO is 63%.

Figure 7 shows the percentage deviation of the proposed technique with ABC, with BFO and with ANFASO methods. Analysis of power generated by battery, MT, PV and WT is analysed in the proposed technique as well as in the ANFASO method. In the proposed method, the maximum power produced by battery, MT, PV and WT is 8 kW, 9.5 kW, 16 kW and 5 kW. The SOC of the proposed technique reaches about 80%. In ANFASO method, the power generated by battery, MT, PV and WT is 7.5 kW, 9 kW, 15 kW and 4.5 kW, respectively. It clearly shows that the proposed method gives maximum power and the total generation cost is also minimum and more efficient. Figure 8 depicts the fitness comparison of the proposed versus existing techniques. The proposed technique converges at the iteration count of 20, and it gives the fitness value from 3 to 0.3. ANFASO converges at the iteration count of 24 and gives the fitness value from 3.4 to 0.4. BFO converges at the iteration count of 36 and gives the fitness value from 3.5 to 0.5. ABC converges at the iteration count of 38 and gives the fitness value from 4.2 to 0.6. The computation time and total generation cost are evaluated and compared with the ABC, BFO and ANFASO methods to evaluate the proposed method effectiveness. Finally, it clearly shows that the proposed method gives better results when compared to ANFASO method.

## 5 Conclusion

In this paper, a hybrid technique is introduced for system modelling and management of MG-connected systems with low cost. The proposed hybrid approach is based on the

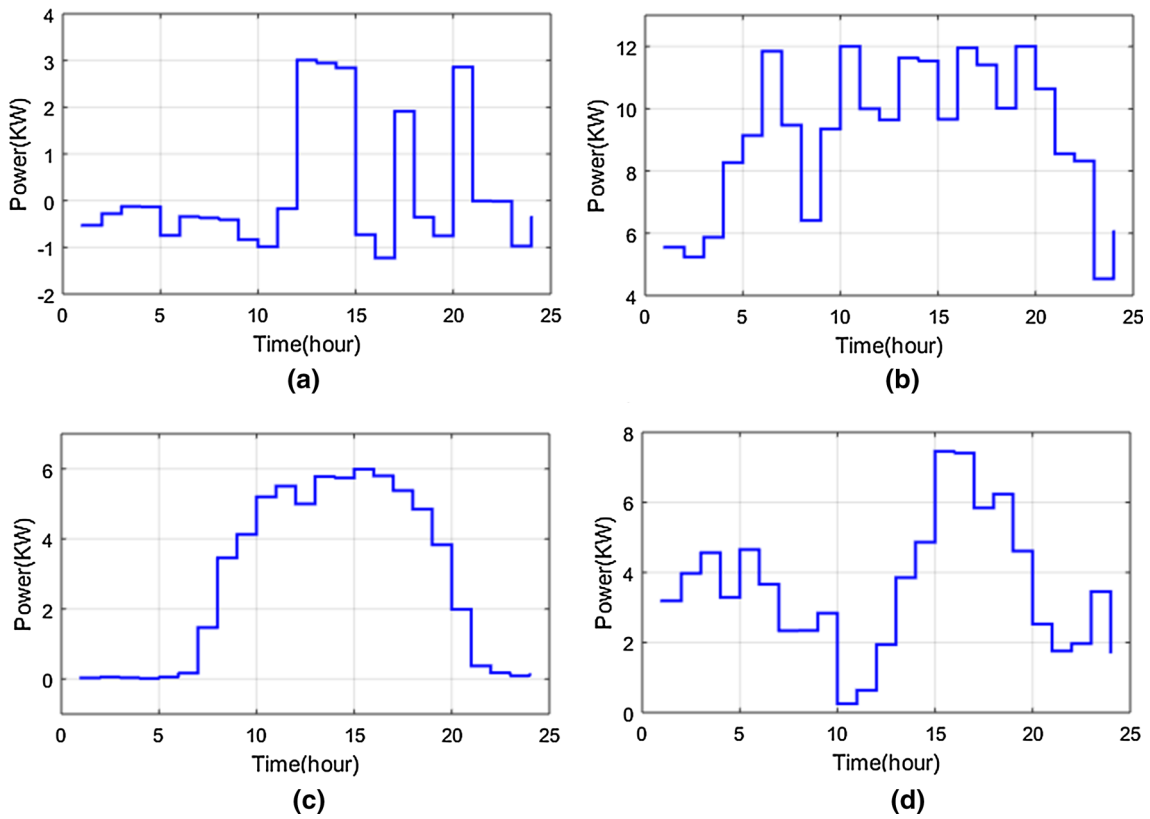


Fig. 3 Analysis of power generated by a battery, b MT, c PV, d WT using the proposed method

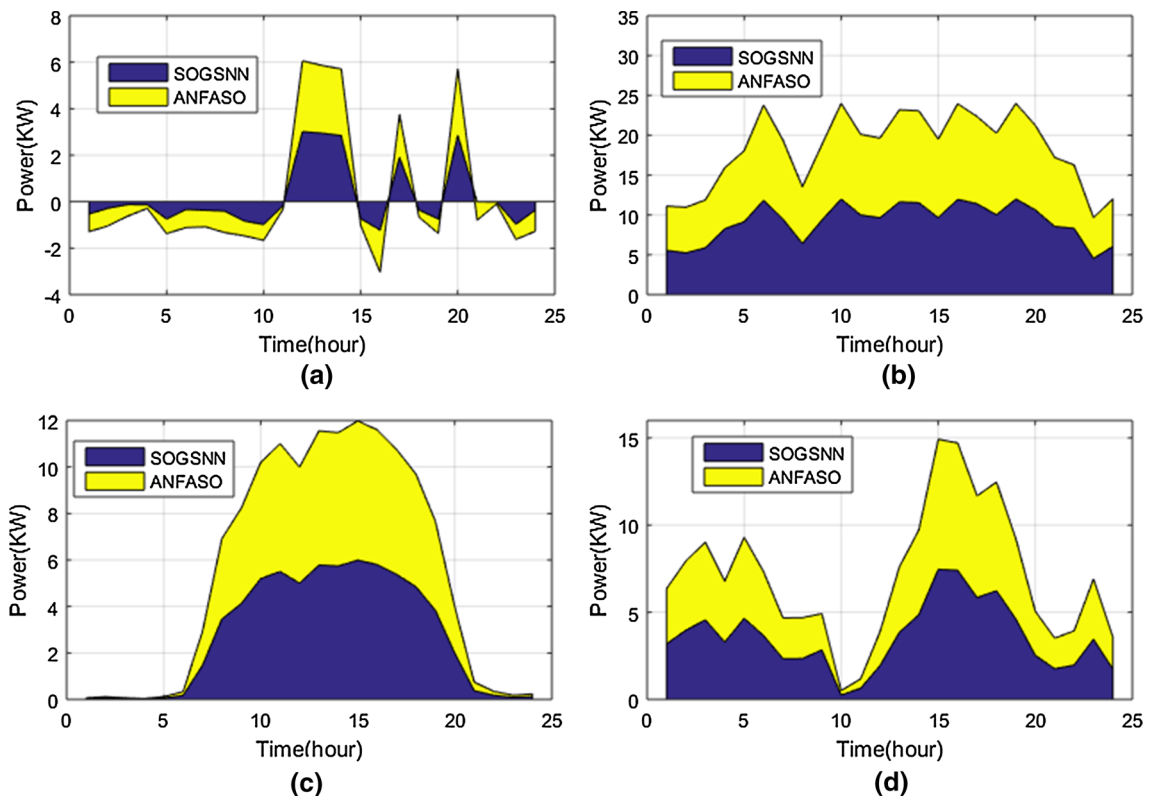
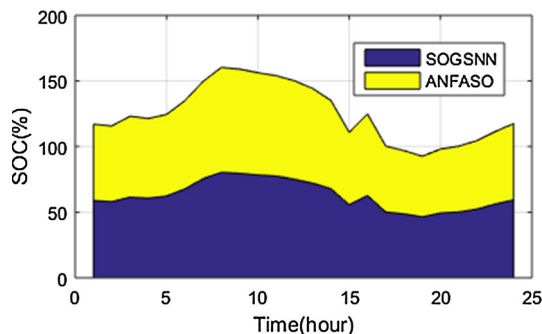


Fig. 4 Analysis of power generated by a battery, b MT, c PV (d) WT using the proposed and ANFASO methods



**Fig. 5** Analysis of SOC (%) using the proposed and ANFASO methods

combination of GSA-ANN and SSA. The objective of the proposed approach is to minimize the fuel cost, to reduce the emission and operating and maintenance costs and also to better utilize the renewable energy resources. The optimization problem includes a variety of energy sources that are likely to be found in the micro-grid, such as PV system, MT system, WT system and battery storage. Constraint functions are added to the optimization problem to reflect some of the additional considerations often found in a small-scale generation system. From the results obtained, it

**Table 3** Comparison analysis of elapsed time of the proposed technique with ANFASO technique

Solution techniques	Time in seconds
ABC	37.11
BFO (Su et al. 2014)	36.96
ANFASO	38.08
Proposed	36.47

is clear that from the optimal power operating costs and utilization of energy sources for the MG the optimization works very well and can give the optimal power strategy to the generators after taking into account the objective functions. The proposed hybrid technique is executed in MATLAB/Simulink working platform, and their performance level is tested. The performance of the proposed hybrid technique is compared with that of other solution techniques like ANFASO method. The comparison result reveals the superiority of the proposed technique and confirms its potential to solve the problem. The proposed method has less CPU time when compared with other techniques like ANFASO method. The comparative results prove that the proposed method is highly competent over

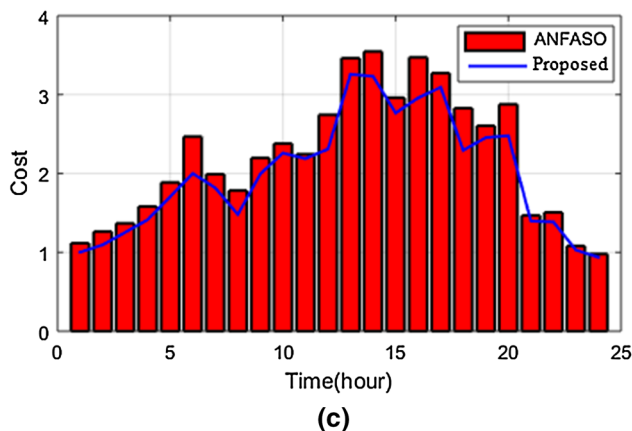
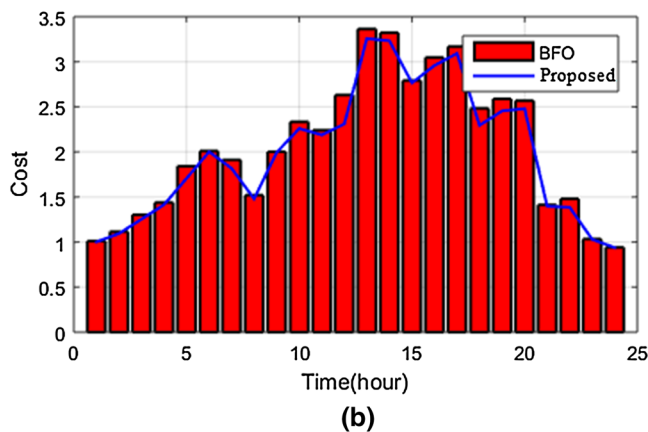
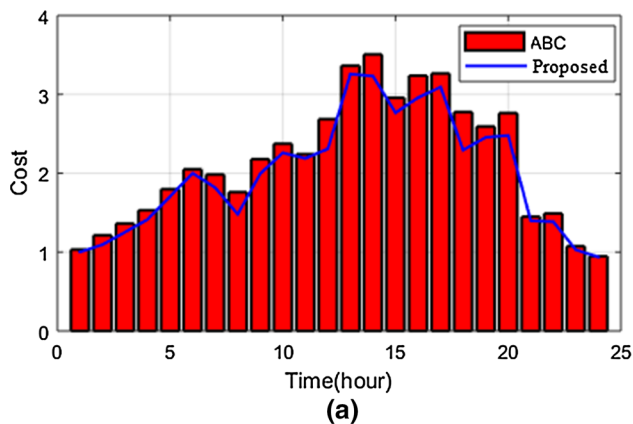


**Fig. 6** Cost analysis of the proposed with existing techniques **a** ABC–proposed, **b** BFO–proposed, **c** ANFASO–proposed

**Table 4** Statistical analysis of market clearing price (MCP) of the proposed and ANFASO techniques

Market clearing price (MCP %)			
Techniques	Mean	Median	SD
ABC	2.151	2.115	0.799
BFO	2.065	2.005	0.768
ANFASO	2.211	2.221	0.818
Proposed	1.991	1.998	0.735

**Table 5** Performance comparison of the different techniques

Solution techniques	Best	Worst	ECAP
ABC	0.72	4.16	4.77
BFO	0.63	3.95	5.26
ANFASO	0.55	3.70	5.72
Proposed	0.31	3.49	10.25

**Table 6** Comparison analysis of SoC using various methods

SoC (%)			
Solution techniques	ABC	BFO	ANFASO
Proposed technique	ABC	BFO	ANFASO
82%	78%	70%	63%

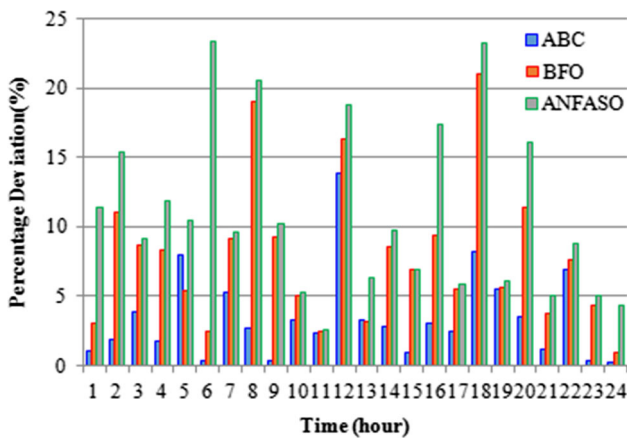


**Fig. 7** Percentage deviation of the proposed with the existing techniques

the other existing techniques. The future scope of hybrid power generation system is to develop huge model by producing the power in MW or GW to fulfil the electricity requirement of an urban and rural areas for a day. We can generate the large amount of power from the renewable energy sources into future by using the proper location. Many locations or sites are available in India where a large potential of wind and solar energy is available. From this

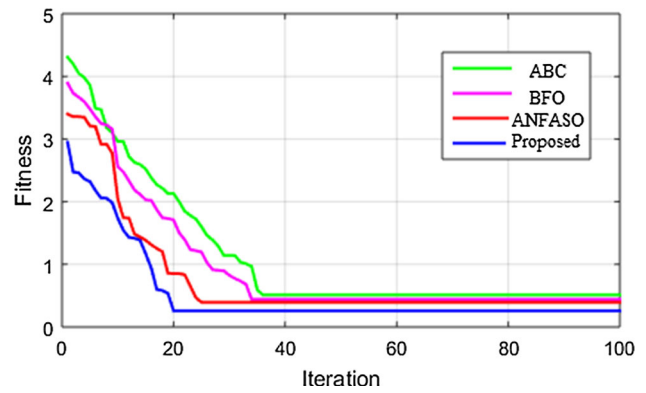


**Fig. 8** Convergence characteristics of the proposed and existing techniques

study, we can design the hybrid power system which fulfils the load requirement of the consumer in rural areas where electricity is not in approach, i.e. hilly area of the world. Also, we can reduce the pollution and fulfil the power demand into the future. The future research includes implementing more tests on real-time basis. More intelligent instrumentation may be utilized to get optimized system in terms of efficiency and cost.

**Funding** No funding has been received.

**Compliance with ethical standards**

**Conflict of interest** The authors declare that they have no conflict of interest.

**Ethical approval** This article does not contain any studies with human participants performed by any of the authors.

**References**

Aghajani G, Ghadimi N (2018) Multi-objective energy management in a micro-grid. *Energy Rep* 4:218–225. <https://doi.org/10.1016/j.egy.2017.10.002>

Ahmed N, Miyatake M, Al-Othman A (2008) Power fluctuations suppression of stand-alone hybrid generation combining solar photovoltaic/wind turbine and fuel cell systems. *Energy Convers Manag* 49:2711–2719. <https://doi.org/10.1016/j.enconman.2008.04.005>

Aktas A, Erhan K, Özdemir S, Özdemir E (2018) Dynamic energy management for photovoltaic power system including hybrid energy storage in smart grid applications. *Energy* 162(72–82):2018. <https://doi.org/10.1016/j.energy.2018.08.016>

Aktas A, Erhan K, Ozdemir S, Ozdemir E (2019) Experimental investigation of a new smart energy management algorithm for a hybrid energy storage system in smart grid applications. *Electr Power Syst Res* 144:185–196. <https://doi.org/10.1016/j.epr.2016.11.022>

Bajpai P, Dash V (2012) Hybrid renewable energy systems for power generation in stand-alone applications: a review. *Renew Sustain*



- Energy Rev 16:2926–2939. <https://doi.org/10.1016/j.rser.2012.02.009>
- Dali M, Belhadj J, Roboam X (2010) Hybrid solar–wind system with battery storage operating in grid-connected and standalone mode: control and energy management – Experimental investigation. *Energy* 35:2587–2595. <https://doi.org/10.1016/j.energy.2010.03.005>
- Deshmukh M, Deshmukh S (2008) Modeling of hybrid renewable energy systems. *Renew Sustain Energy Rev* 12:235–249. <https://doi.org/10.1016/j.rser.2006.07.011>
- Dursun E, Kilic O (2012) Comparative evaluation of different power management strategies of a stand-alone PV/Wind/PEMFC hybrid power system. *Int J Electr Power Energy Syst* 34:81–89. <https://doi.org/10.1016/j.ijepes.2011.08.025>
- Elsied M, Oukaour A, Gualous H, Lo Brutto O (2016) Optimal economic and environment operation of micro-grid power systems. *Energy Convers Manag* 122:182–194. <https://doi.org/10.1016/j.enconman.2016.05.074>
- Figueiredo J, Martins J (2010) Energy production system management—renewable energy power supply integration with building automation system. *Energy Convers Manag* 51:1120–1126. <https://doi.org/10.1016/j.enconman.2009.12.020>
- Golsorkhi M, Lu D (2015) A control method for inverter-based islanded microgrids based on V–I droop characteristics. *IEEE Trans Power Deliv* 30:1196–1204. <https://doi.org/10.1109/tpwrd.2014.2357471>
- Goroohi Sardou I, Zare M, Azad-Farsani E (2018) Robust energy management of a microgrid with photovoltaic inverters in VAR compensation mode. *Int J Electr Power Energy Syst* 98:118–132. <https://doi.org/10.1016/j.ijepes.2017.11.037>
- Gu W, Wu Z, Bo R et al (2014) Modeling, planning and optimal energy management of combined cooling, heating and power microgrid: a review. *Int J Electr Power Energy Syst* 54:26–37. <https://doi.org/10.1016/j.ijepes.2013.06.028>
- Hajizadeh A, Golkar M (2007) Intelligent power management strategy of hybrid distributed generation system. *Int J Electr Power Energy Syst* 29:783–795. <https://doi.org/10.1016/j.ijepes.2007.06.025>
- Indragandhi V, Logesh R, Subramaniaswamy V, Vijayakumar V, Siarry P, Uden L (2018) Multi-objective optimization and energy management in renewable based AC/DC microgrid. *Comput Electr Eng*. <https://doi.org/10.1016/j.compeleceng.2018.01.023>
- Jain M, Singh V, Rani A (2018) A novel nature-inspired algorithm for optimization: squirrel search algorithm. *Swarm Evolut Comput*. <https://doi.org/10.1016/j.swevo.2018.02.013>
- Kaundinya D, Balachandra P, Ravindranath N (2009) Grid-connected versus stand-alone energy systems for decentralized power—a review of literature. *Renew Sustain Energy Rev* 13:2041–2050. <https://doi.org/10.1016/j.rser.2009.02.002>
- Luna A, Meng L, Diaz N et al (2018) Online energy management systems for microgrids: experimental validation and assessment framework. *IEEE Trans Power Electron* 33:2201–2215. <https://doi.org/10.1109/tpel.2017.2700083>
- Mohamed F, Koivo H (2007) System modelling and online optimal management of microgrid with battery storage. *Renew Energy Power Qual J* 1:74–78. <https://doi.org/10.24084/repqj05.220>
- Moradi M, Foroutan V, Abedini M (2017) Power flow analysis in islanded micro-grids via modeling different operational modes of DGs: a review and a new approach. *Renew Sustain Energy Rev* 69:248–262. <https://doi.org/10.1016/j.rser.2016.11.156>
- Moradi H, Esfahanian M, Abtahi A, Zilouchian A (2018) Optimization and energy management of a standalone hybrid microgrid in the presence of battery storage system. *Energy* 147:226–238. <https://doi.org/10.1016/j.energy.2018.01.016>
- Morstyn T, Hredzak B, Aguilera R, Agelidis V (2018) Model predictive control for distributed microgrid battery energy storage systems. *IEEE Trans Control Syst Technol* 26:1107–1114. <https://doi.org/10.1109/tcst.2017.2699159>
- Muralitharan K, Sakthivel R, Vishnuvarthan R (2018) Neural network based optimization approach for energy demand prediction in smart grid. *Neurocomputing* 273:199–208. <https://doi.org/10.1016/j.neucom.2017.08.017>
- Najafzadeh K, Heydari H (2012) New inverter fault current limiting method by considering microgrid control strategy. *Adv Mater Res* 463–464:1647–1653. <https://doi.org/10.4028/www.scientific.net/amr.463-464.1647>
- Palizban O, Kauhaniemi K, Guerrero J (2014) Microgrids in active network management—part I: hierarchical control, energy storage, virtual power plants, and market participation. *Renew Sustain Energy Rev* 36:428–439. <https://doi.org/10.1016/j.rser.2014.01.016>
- Pavan Kumar Y, Ravikumar B (2016) A simple modular multilevel inverter topology for the power quality improvement in renewable energy based green building microgrids. *Electr Power Syst Res* 140:147–161. <https://doi.org/10.1016/j.epsr.2016.06.027>
- Prakash S, Sinha S (2014) Simulation based neuro-fuzzy hybrid intelligent PI control approach in four-area load frequency control of interconnected power system. *Appl Soft Comput* 23:152–164. <https://doi.org/10.1016/j.asoc.2014.05.020>
- Rashedi E, Nezamabadi-pour H, Saryazdi S (2009) GSA: a gravitational search algorithm. *Inf Sci* 179:2232–2248. <https://doi.org/10.1016/j.ins.2009.03.004>
- Roy K, Mandal K (2014) Hybrid optimization algorithm for modeling and management of micro grid connected system. *Front Energy* 8:305–314. <https://doi.org/10.1007/s11708-014-0308-8>
- Roy K, Mandal K, Mandal A (2016) Modeling and managing of micro grid connected system using improved artificial bee colony algorithm. *Int J Electr Power Energy Syst* 75:50–58. <https://doi.org/10.1016/j.ijepes.2015.08.003>
- Roy K, Krishna Mandal K, Chandra Mandal A, Narayan Patra S (2018) Analysis of energy management in micro grid—a hybrid BFOA and ANN approach. *Renew Sustain Energy Rev* 82:4296–4308. <https://doi.org/10.1016/j.rser.2017.07.037>
- Sharma S, Bhattacharjee S, Bhattacharya A (2018) Probabilistic operation cost minimization of micro-grid. *Energy* 148:1116–1139. <https://doi.org/10.1016/j.energy.2018.01.164>
- Su W, Wang J, Roh J (2014) Stochastic energy scheduling in microgrids with intermittent renewable energy resources. *IEEE Trans Smart Grid* 5:1876–1883. <https://doi.org/10.1109/tsg.2013.2280645>
- Thao N, Uchida K (2016) A control strategy based on fuzzy logic for three-phase grid-connected photovoltaic system with supporting grid-frequency regulation. *J Autom Control Eng* 4:96–103. <https://doi.org/10.12720/joace.4.2.96-103>
- Vasquez JC, Guerrero JM, Miret J, Castilla M, De Vicuna LG (2010) Hierarchical control of intelligent microgrids. *IEEE Ind Electron Mag* 4:23–29. <https://doi.org/10.1109/mie.2010.938720>
- Yi Z, Dong W, Etemadi A (2018) A unified control and power management scheme for PV-battery-based hybrid microgrids for both grid-connected and islanded modes. *IEEE Trans Smart Grid* 9:5975–5985. <https://doi.org/10.1109/tsg.2017.2700332>

**Publisher's Note** Springer Nature remains neutral with regard to jurisdictional claims in published maps and institutional affiliations.